

# **NUMERICAL SIMULATION OF OPTICAL PROPERTIES OF PLASMONIC METAL NANOSTRUCTURES**

**SANGITA**



**CENTRE FOR ENERGY STUDIES  
INDIAN INSTITUTE OF TECHNOLOGY DELHI**

**OCTOBER 2017**

© Indian Institute of Technology Delhi (IITD), New Delhi, 2017

# **NUMERICAL SIMULATION OF OPTICAL PROPERTIES OF PLASMONIC METAL NANOSTRUCTURES**

by

**SANGITA**

**CENTRE FOR ENERGY STUDIES**

*Submitted*

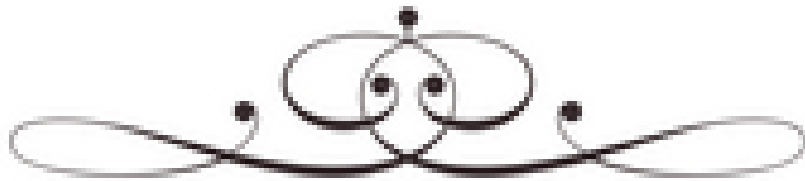
*In fulfillment of the requirements of the degree of Doctor of Philosophy*

to the



**Indian Institute of Technology Delhi**

**October 2017**



*Dedicated to*  
*My Late Parents*

## **CERTIFICATE**

This is to certify that the thesis entitled “**Numerical Simulation of Optical Properties of Plasmonic Metal Nanostructures**” being submitted by Sangita to the **Indian Institute of Technology Delhi** is worthy of consideration for the award of the degree of ‘**Doctor of Philosophy**’ in Centre for Energy Studies, and is a record of bonafide research work carried out by her. Sangita has worked under my guidance and supervision and the results contained in this work have not been submitted in part or full to any other university or institute for award of any degree. I approve the thesis for the award of the aforesaid degree.

Date:

New Delhi

Dr. R. P. Sharma

Professor

Centre for Energy Studies

Indian Institute of Technology Delhi

Dr. R Uma

Associate Professor

Centre for Energy Studies

Indian Institute of Technology Delhi

## **ACKNOWLEDGEMENTS**

Today I am writing this note of thanks is the finishing touch on my thesis. It has been a period of intense learning for me, not only in the scientific arena, but also on a personal level. I would like to give reflections on those persons who supported me throughout this period.

It is an honour for me to express a deep sense of gratitude and profound indebtedness towards my thesis supervisor Professor R. P. Sharma, Centre for Energy Studies, IIT Delhi, for his invaluable assistance, constant support, guidance, and encouragement. He has always provided proactive interventions whenever things got stuck or deviated. It was my prerogative to have his insightful advice and enriching feedback during my course of research work. I could not have imagined having a better advisor and mentor for my Ph.D. work. It is because of his deep knowledge of the subject that this work has taken the present shape.

I am grateful to my supervisor Dr. R. Uma, Associate Professor, Centre for Energy Studies, IIT Delhi, for her generous support and guidance throughout my Ph.D. work. I wish to express my sincere thanks to Dr. Vamsi Krishna, Prof. Viresh Dutta, Prof. T. S. Bhatti, Prof. A.D. Rao and all faculty members of CES for their valuable suggestions, feedbacks and approval of my thesis work. I thank to other staff members of Center for Energy studies, IIT Delhi for their kind help and cooperation during my research work.

I take this opportunity to thank my lab-mates, Dr. Alok, Dr. Monika, Dr. Naveen, Dr. Nitin, Dr. Nidhi, Dr. Nilesh, Dr. Ramkishore, Dr. Hardik, Dr. Anju, Dr. Ashish, Dr. Swati, Dr. Ravinder, Richa, Prachi, Neha, Pradeep, Piyush, Shivani, Gyanendra, Rajesh, Saba, Sintu and Parineet for their cooperation and support during my research work.

Special thanks to my friends Saurabh Srivastava, Sachin Chauhan, Sapna Mudgal, Preetam Singh, Dinesh Sharma and Manisha Singh for their sincere encouragement and support throughout my thesis writing.

It's my fortune to gratefully acknowledge the support of my best friends, Charu Dwivedi, Deepika Singh and Preeti Teotia for their unconditional support and generous care in every phase of my life.

This acknowledgement would remain incomplete without expressing my heartfelt feelings towards my bhaiya and bhabhi who have always been like my parents and never made me feel their absence. Deepest thanks to my family members especially bhabhi and sisters for their love, encouragement and constant support without which I would not have been able to handle the toughest phase of my life. I am in short of words for my younger brother Raju who is a constant motivation and like a backbone for me. I take immense pleasure to acknowledge my In-laws Dr. D. V. Singh and Smt. Rajesh and other family members Ruchi, Arun Bhaiya and Monika for motivating me to pursue my dreams.

I owe thanks to a very special person, my husband, my soul mate, Shagun Kumar Roopak, for his continued and unfailing love, support and understanding during my pursuit of Ph.D. degree that made the completion of thesis possible. You were always around at times I thought that it is impossible to continue, you helped me to keep things in perspective. I greatly value his contribution and deeply appreciate his belief in me.

Last but not the least; I solicit blessings of God for progress and prosperity.

***Sangita***

## **ABSTRACT**

Metallic nanoparticles are the building blocks for the emergent field of plasmonics that has revolutionized the field of photonics by giving the ability to manipulate the light at nano scale and overcoming the resolution limits of conventional optics. Metal nanoparticles support surface plasmon resonances that have wide tunability in different realm of electromagnetic spectrum. The focus of this work lies on the description of metallic nanoparticles – their optical response, how their size, shape, material composition, surrounding medium, presence of another nanoparticle plays a crucial role to affect the resonance. Numerical simulations of the absorption, scattering and extinction efficiencies have been performed using the discrete dipole approximation (DDA) method.

In order to accomplish the motive of the present work, numerical simulations have been done for plasmonically coupled homodimer and heterodimer systems. Plasmon coupling has been a great approach to tune the surface plasmon resonance into the desired wavelength of the optical spectrum. To reveal the plasmonic effects in a coupled system, homodimer and heterodimer cases are compared with the monomer. Further, core shell nanogeometry has been chosen to observe the broad-band plasmonic effect. It was accounted that core shell nanospheroid is more appropriate nanogeometry as compared to core shell nanosphere and simply nanospheroid in terms of wide tunability of surface plasmon resonance. This wide tunability (400-1100nm) of surface plasmon resonance could be utilized to increase the red response of the Si solar cell where it is a poor absorber.



Surface plasmon effects of various metal nanostructures (sphere, oblate spheroid, cylinder and rectangular) embedded in perovskite (methyl ammonium lead iodide) medium have been analyzed for better light incoupling. Spatial field distribution analysis primarily elucidates that rectangular shape is more promising as the oscillating charge confinement is high at the corners. This study gives an insight for the upcoming improvement of perovskite based photovoltaics due to the plasmon induced light incoupling to the host medium near the band edge. Further, plasmonic effects in hexagonal nanoprism (HNP) embedded in different inorganic medium have been explored in context of broadband tunability. Large structural anisotropy allows to observe in-plane and out of plane resonances in the optical spectrum. In addition, broadband plasmonic resonances have been discussed in organic (P3HT: PCBM blend) medium by employing triangular nanoprism for improved light incoupling into organic medium. This broadband tunability may be utilized to achieve cost effective organic solar cells.

The present study gives an insight to cognize the plasmonic resonance tunability in promising metallic nanogeometries in different dielectric environments that could be helpful for the scientific community in context of improved photovoltaics and many other applications in different domain of electromagnetic spectrum.

सार

मैटेलिक (धात्विक) नैनो पार्टिकल्स प्लाज़्मोनिक्स के आधुनिक क्षेत्र के लिए मूल ब्लॉक हैं जिसने नैनो पैमाने पर प्रकाश को मैनिपुलेट करने की क्षमता देकर और पारंपरिक प्रकाशिकी के रेजोलुशन सीमाओं पर काबू पाकर फोटोनिक्स के क्षेत्र में क्रांति ला दी है। मेटल नैनो पार्टिकल्स सरफेस (सतह) प्लाज़्मोन रेजोनेंस (अनुनाद) को सपोर्ट करते हैं जिसमें विद्युत चुम्बकीय स्पेक्ट्रम के विभिन्न क्षेत्र की व्यापक ट्यूनेबिलिटी होती है। इस काम का फोकस निम्न पर है- मेटल नैनो पार्टिकल्स का वर्णन, उनकी ऑप्टिकल प्रतिक्रिया, निम्न नैनो पार्टिकल्स का आकार, शेप, मटेरियल संरचना, आसपास के माध्यम, दूसरे नैनो पार्टिकल की उपस्थिति अनुनाद को प्रभावित करने के लिए महत्वपूर्ण भूमिका निभाते हैं। अवशोषण, स्कैटरिंग और एक्सटिंक्शन (विलुप्त) क्षमताओं का न्यूमेरिकल (संख्यात्मक) सिमुलेशन, डिस्क्रीट (असतत) द्विध्रुव अप्रोक्सिमेशन (सन्निकटन) (डी.डी.ए.) विधि का उपयोग करते हुए किया गया है।

वर्तमान कार्य के उद्देश्य को पूरा करने के लिए प्लाज़्मोनीकली कपलड (युग्मित) होमोडाइमर और हेट्रोडाइमर सिस्टम का न्यूमेरिकल सिमुलेशन किया गया है। सरफेस प्लाज़्मोन रेजोनेंस को ऑप्टिकल स्पेक्ट्रम के वांछित वेवलेंथ (तरंग दैर्घ्य) में ट्यून (धुन) करने के लिए प्लाज़्मोन कपलिंग एक महान तरीका है। एक कपलड सिस्टम में प्लाज़्मोनिक इफेक्ट्स (प्रभाव) प्रकट करने के लिए होमोडाइमर और हेट्रोडाइमर की तुलना मोनोमर से की जाती है। इसके अलावा, कोर शैल नैनो ज्योमेट्री (ज्यामिति) को ब्रॉड (व्यापक) बैंड प्लाज़्मोनिक इफेक्ट्स का निरीक्षण करने के लिए चुना गया है। यह माना गया था कि सरफेस प्लाज़्मोन रेजोनेंस की विस्तृत ट्यूनेबिलिटी के संदर्भ में कोर शैल नैनो स्फेरोइड ज्योमेट्री, कोर शैल नैनोस्फेयर ज्योमेट्री और साधारण नैनो स्फेरोइड की तुलना में अधिक उपयुक्त है। सरफेस प्लाज़्मोन रेजोनेंस की यह विस्तृत ट्यूनेबिलिटी (400-1100 नैनो मीटर) का उपयोग सिलिकॉन सोलर सेल के रेड (लाल) रेस्पॉन्स (प्रतिक्रिया), जहां यह एक पुअर (कमजोर) अवशोषक है, को बढ़ाने के लिए किया जा सकता है।

बेहतर लाइट कपलिंग के लिए परोव्स्काइट (मिथाइल अमोनियम लेड आयोडाइड) में एम्बेडेड (निहित) विभिन्न मेटल (धातु) नैनोस्ट्रक्चर (गोलाकार, ओब्लैटेक गोलाकार, सिलेंडर और आयताकार) के सरफेस प्लाज़्मोन इफेक्ट्स का विश्लेषण किया गया है। स्पेसियल फील्ड डिस्ट्रीब्यूशन (वितरण) विश्लेषण मुख्य रूप से स्पष्ट करता है कि आयताकार आकार कोनों पर औसिलेटिंग चार्ज कन्फ़ाइनमेंट को उच्च करने के लिए अधिक आशाजनक है। यह अध्ययन, परोव्स्काइट आधारित फोटोवोल्टाईक की आगामी सुधार के लिए प्लाज़्मोन प्रेरित लाइट कपलिंग के कारण होस्ट मीडियम (माध्यम) में बैंड की ऐज के पास एक अंतर्दृष्टि देता है। इसके अलावा, ब्रॉडबैंड ट्यूनेबिलिटी के संदर्भ में विभिन्न अकार्बनिक माध्यमों में एम्बेडेड (निहित) हेक्सागोनल नैनोप्रिज्म (एच.एन.पी.) में प्लाज़्मोनिक इफेक्ट्स की खोज की गई है। लार्ज (बड़ी) स्ट्रक्चरल (संरचनात्मक) एनआईसोट्रोपी, ऑप्टिकल स्पेक्ट्रम में इन-प्लेन और आउट ऑफ़-प्लेन का निरीक्षण करने की अनुमति देता है। इसके साथ-साथ, कार्बनिक माध्यम में इम्प्रूवड लाइट कपलिंग के लिए ट्राईएंगुलर (त्रिकोणीय) नैनोप्रिज्म को डालकर ब्रॉडबैंड प्लाज़्मोनिक रेजोनेंस की कार्बनिक (P3HT:PCBM मिश्रण) माध्यम में चर्चा की गई है। इस ब्रॉडबैंड ट्यूनेबिलिटी का इस्तेमाल कॉस्ट (लागत) इफेक्टिव कार्बनिक सोलर सेल प्राप्त करने के लिए किया जा सकता है।

वर्तमान अध्ययन, विभिन्न डार्क-इलेक्ट्रिक वातावरण के मैटेलिक (धात्विक) नैनो ज्योमेट्री (ज्यामिति) में प्लाज़्मोनिक रेजोनेंस ट्यूनेबिलिटी जानने के लिए अंतर्दृष्टि प्रदान करता है, जो कि वैज्ञानिक समुदाय के लिए इम्प्रूवड फोटोवोल्टाईक और कई अन्य विद्युत चुम्बकीय स्पेक्ट्रम के विभिन्न डोमेन में अनुप्रयोग के संदर्भ में सहायक हो सकता है।

# **TABLE OF CONTENTS**

<b>CERTIFICATE</b>	i
<b>ACKNOWLEDGEMENTS</b>	ii
<b>ABSTRACT</b>	iv
<b>TABLE OF CONTENTS</b>	vi
<b>LIST OF FIGURES</b>	x
<b>LIST OF TABLES</b>	xviii
<b>ABBREVIATIONS</b>	xix
<b>CHAPTER 1 Introduction</b>	
<b>1.1</b> Surface plasmons-A glorious history	1
<b>1.2</b> Surface plasmons (SPs) in metal nanoparticles	3
<b>1.3</b> Drude-Lorentz- Sommerfeld model	4
<b>1.4</b> Optical properties of spherical nanoparticles	6
<b>1.5</b> Tuning the surface plasmon resonance (SPR)	10
<b>1.5.1</b> Particle size effects	10
<b>1.5.2</b> Shape effects	11
<b>1.5.3</b> Surrounding environments	12
<b>1.5.4</b> Interparticle coupling effects	13
<b>1.6</b> The glamour of plasmonics	15
<b>1.6.1</b> Plasmonics in photovoltaics	15
<b>1.7</b> Plasmonic materials	16

<b>1.8</b>	Methodology	18
<b>1.8.1</b>	Quasi-static approximation	18
<b>1.8.2</b>	Mie theory-electrodynamic approach	19
<b>1.8.3</b>	Numerical approach	19
<b>1.8.3.1</b>	Discrete dipole approximation	20
<b>1.8.3.1.1</b>	Applicability of DDA	22
<b>1.8.3.1.2</b>	Memory and CPU requirements	23
<b>1.9</b>	Thesis organization	24
	Reference	27
<b>CHAPTER 2 Numerical simulation of extinction spectra of plasmonically coupled nanospheres using discrete dipole approximation: Influence of compositional asymmetry</b>		
<b>2.1</b>	Introduction	31
<b>2.2</b>	Computational method	35
<b>2.3</b>	Results and discussion	36
<b>2.4</b>	Conclusions	44
	References	46
<b>CHAPTER 3 Numerical Simulation of Broadband Scattering by Coated and Noncoated Metal Nanostructures Using Discrete Dipole Approximation Methods</b>		
<b>3.1</b>	Introduction	49
<b>3.2</b>	Computational Method	51
<b>3.3</b>	Results and discussion	52
<b>3.4</b>	Conclusions	60
	References	61

**CHAPTER 4 Light incoupling tolerance of resonant and nonresonant metal nanostructures embedded in perovskite medium: Effect of various geometries on broad spectral resonance**

4.1 Introduction	63
4.2 Computational method	66
4.3 Results and discussion	67
4.4 Conclusions	84
References	85

**CHAPTER 5 Hexagonal Nanoprism for Broadband Tunability: Ultraviolet to Infrared Plasmonics**

5.1 Introduction	87
5.2 Computational method	90
5.3 Photon absorption calculation	91
5.4 Results and discussion	92
5.5 Conclusions	108
References	110

**CHAPTER 6 Broad-Band Light Coupling in Organic Medium by Employing Triangular Nanoprism**

6.1 Introduction	113
6.2 Computational method	115
6.3 Results and discussion	116
6.4 Conclusions	123
6.5 References	124

**CHAPTER 7 Summary and future outlook**

7.1 Summary 126

7.2 Future Outlook 127

**List of Publications** 128

**Bio Data** 131

## List of Figures

<b>Figure Number</b>	<b>Description</b>	<b>Page Number</b>
1.1	The Lycurgus cup shown in (a) reflection and (b) transmission	2
1.2	Interaction of electromagnetic field with Metal nanoparticle	4
1.3	Oscillation of metal plasma in an oscillating external applied field	5
1.4	Metal nanosphere placed into an electrostatic field	7
1.5	Schematic of scattering, absorption and transmission of incident light by a metallic nanosphere	8
1.6	Energy levels of two coupled spherical nanoparticles	14
2.1	Graphical representation of our modelling work: extinction spectra of monomer and touching homodimer and heterodimer of radius 50nm embedded in air	35
2.2	Extinction spectra of various metal nanostructures of radius 50nm embedded in air (a) Ag monomer and touching dimer (b) Au monomer and touching dimer (c) Al monomer and touching dimer	37
2.3	Extinction spectra of various metal nanostructures of radius 50nm embedded in air (a) Ag and Au monomer and touching Au-Ag heterodimer (b) Au and Al monomer and touching Au-Al heterodimer (c) Ag and Al monomer and touching Ag-Al heterodimer	38

<b>2.4</b>	Simulated extinction spectra of various homodimer of radius 50nm embedded in air with varying particle edge-edge separation (a) Ag-Ag homodimer (b) Au-Au homodimer (c) Al-Al homodimer	39
<b>2.5</b>	Simulated extinction spectra of various monomers of varying size embedded in air (a) Ag monomer (b) Au monomer (c) Al monomer	41
<b>2.6</b>	Simulated extinction spectra of various touching homodimer of varying size embedded in air (a) Ag-Ag homodimer (b) Au-Au homodimer (c) Al-Al homodimer	43
<b>2.7</b>	Simulated extinction spectra of various touching heterodimers of varying size embedded in air (a) Au-Ag heterodimer (b) Au-Al heterodimer (c) Ag-Al heterodimer	44
<b>3.1</b>	Schematic diagram of coated and noncoated nanostructures and their optical spectra with effective radii =80 nm	53
<b>3.2</b>	(a) Scattering (b) Absorption spectra of core shell (Au@SiO <sub>2</sub> ) nanospheroid with $a_{\text{eff}}=50$ nm for different aspect ratio (0.1 to 0.6)	54
<b>3.3</b>	(a) Scattering (b) Absorption spectra of core shell (Au@SiO <sub>2</sub> ) nanospheroid with $a_{\text{eff}}=60$ nm for different aspect ratio (0.1 to 0.6)	55
<b>3.4</b>	(a) Scattering (b) Absorption spectra of core shell (Au@SiO <sub>2</sub> ) nanospheroid with $a_{\text{eff}}=70$ nm for different aspect ratio (0.1 to 0.6)	56
<b>3.5</b>	(a) Scattering (b) Absorption spectra of core shell (Au@SiO <sub>2</sub> ) nanospheroid with $a_{\text{eff}}=80$ nm for different aspect ratio (0.1 to 0.6)	57
<b>3.6</b>	(a) Scattering (b) Absorption spectra of core shell (Au@SiO <sub>2</sub> )	58



	nanospheroid with $a_{\text{eff}}=90$ nm for different aspect ratio (0.1 to 0.6)	
<b>3.7</b>	(a) Scattering (b) Absorption spectra of core shell (Au@SiO <sub>2</sub> ) nanosphere for different $a_{\text{eff}}$ ranging from 40 to 100 nm	59
<b>3.8</b>	(a) Scattering (b) absorption spectra of noncoated Au nanospheroid for different size with fixed aspect ratio 0.1	59
<b>4.1</b>	Optical properties of the CH <sub>3</sub> NH <sub>3</sub> PbI <sub>3</sub> perovskite (a) Real (n) and imaginary (k) part of refractive index (b) absorption coefficient of perovskite material	67
<b>4.2</b>	Graphic representation of the modelling approach showing extinction spectra of various possible nanostructures (sphere, oblate spheroid with aspect ratio 0.6, cylinder having length and diameter 75nm and 44nm respectively, rectangular box with the sides 1:2:2) of effective radii 30nm embedded in perovskite medium (a) Au (b) Ag (c) Al	68
<b>4.3</b>	Electric field intensity of various possible nanostructures of Au of effective radii 30nm embedded in perovskite medium (a) sphere (b) oblate spheroid with aspect ratio 0.6 (c) cylinder having length and diameter 75nm and 44nm respectively (d) rectangular box with the sides 1:2:2	71
<b>4.4</b>	Electric field intensity of various possible nanostructures of Ag of effective radii 30nm embedded in perovskite medium (a) sphere (b) oblate spheroid with aspect ratio 0.6 (c) cylinder having length and	72

	diameter 75nm and 44nm respectively (d) rectangular box with the sides 1:2:2	
<b>4.5</b>	Electric field intensity of various possible nanostructures of Al of effective radii 30nm embedded in perovskite medium (a) sphere (b) oblate spheroid with aspect ratio 0.6 (c) cylinder having length and diameter 75nm and 44nm respectively (d) rectangular box with the sides 1:2:2	73
<b>4.6</b>	Extinction spectra of nano oblates ( $a_{eff}=30nm$ , $aspr=0.6$ ) as a function of wavelength for discretization of dipole (8528-314504) (a) Au (b) Ag (c) Al	74
<b>4.7</b>	Extinction spectra of various nano oblate spheroids for varying size with aspect ratio 0.1 embedded in perovskite medium (a) Au (b) Ag (c) Al	75
<b>4.8</b>	Three dimensional view of electric field intensity of various nano oblate spheroids ( $a_{eff}=60nm$ ) with aspect ratio 0.1 embedded in perovskite medium (a) Au (b) Ag (c) Al	77
<b>4.9</b>	Simulated extinction spectra of various nano oblate spheroids for varying size with aspect ratio 0.3 embedded in perovskite medium (a) Au (b) Ag (c) Al	78
<b>4.10</b>	Three dimensional representation of electric field intensity of various nano oblate spheroids ( $a_{eff}=60nm$ ) with aspect ratio 0.3 embedded in perovskite medium (a) Au (b) Ag (c) Al	79

<b>4.11</b>	Simulated extinction spectra of various nano oblate spheroids for varying size with aspect ratio 0.6 embedded in perovskite medium (a) Au (b) Ag (c) Al	80
<b>4.12</b>	Three dimensional electric field intensity of various nano oblate spheroids (a <sub>eff</sub> =60nm) with aspect ratio 0.6 embedded in perovskite medium (a) Au (b) Ag (c) Al	81
<b>4.13</b>	Simulated extinction spectra of various nano oblate spheroids for varying size with aspect ratio 0.9 embedded in perovskite medium (a) Au (b) Ag (c) Al	82
<b>4.14</b>	Three dimensional electric field intensity of various nano oblate spheroids (a <sub>eff</sub> =60nm) with aspect ratio 0.9 embedded in perovskite medium (a) Au (b) Ag (c) Al	83
<b>5.1</b>	Graphic representation of HNP of varying hexagonal side (10nm-50nm) with prism height 50nm and their corresponding extinction spectra	90
<b>5.2</b>	Absorption/Scattering/Extinction efficiency of Au HNP for varying hexagonal side from 10nm to 50nm at constant prism height (20nm, 50nm and 80nm) as row- wise embedded in silica matrix	93
<b>5.3</b>	Absorption/Scattering/Extinction efficiency of Ag HNP for varying hexagonal side from 10nm to 50nm at constant prism height (20nm, 50nm and 80nm) as row- wise embedded in silica matrix	95
<b>5.4</b>	Absorption/Scattering/Extinction efficiency of Al HNP for varying	96

	hexagonal side from 10nm to 50nm at constant prism height (20nm, 50nm and 80nm) as row- wise embedded in silica matrix	
<b>5.5</b>	Absorption/Scattering/Extinction efficiency of Au HNP for varying hexagonal side from 10nm to 50nm at constant prism height (20nm, 50nm and 80nm) as row- wise embedded in TiO <sub>2</sub> matrix	97
<b>5.6</b>	Absorption /Scattering/Extinction efficiency of Ag HNP for varying hexagonal side from 10nm to 50nm at constant prism height (20nm, 50nm and 80nm) as row- wise embedded in TiO <sub>2</sub> matrix	98
<b>5.7</b>	Absorption/Scattering/Extinction efficiency of Al HNP for varying hexagonal side from 10nm to 50nm at constant prism height (20nm, 50nm and 80nm) as row- wise embedded in TiO <sub>2</sub> matrix	99
<b>5.8</b>	Absorption/Scattering/Extinction efficiency of Au HNP for varying hexagonal side from 10nm to 50nm at constant prism height (20nm, 50nm and 80nm) as row- wise embedded in Si matrix	100
<b>5.9</b>	Absorption/Scattering/Extinction efficiency of Ag HNP for varying hexagonal side from 10nm to 50nm at constant prism height (20nm, 50nm and 80nm) as row- wise embedded in Si matrix	102
<b>5.10</b>	Absorption/Scattering/Extinction efficiency of Al HNP for varying hexagonal side from 10nm to 50nm at constant prism height (20nm, 50nm and 80nm) as row- wise embedded in Si matrix	103
<b>5.11</b>	Three dimensional electric field distributions around Au HNPs embedded in Si at constant prism height 50nm and varying	104

	hexagonal side (a) 10nm (b) 30nm (c) 50nm	
<b>5.12</b>	Three dimensional electric field distributions around Au HNPs embedded in Si matrix at constant hexagonal side 50nm and varying prism height (a) 20nm (b) 50nm (c) 80nm	105
<b>5.13</b>	Three dimensional electric field distributions around (a) Au (b) Ag (c) Al HNP embedded in Si matrix with hexagonal side and prism height 50nm	106
<b>5.14</b>	Three dimensional electric field distributions around Au HNP of hexagonal side 30nm and prism height 80nm embedded in (a) Silica (b) TiO <sub>2</sub> (c) Si	107
<b>5.15</b>	Absorption of photons in a thin silicon film with and without NPs under AM 1.5	108
<b>6.1</b>	Absorption efficiency of Al nanoprism for varying prism height (5-40nm) at constant edge length 50nm	116
<b>6.2</b>	Absorption efficiency of Al nanoprism for varying prism height (5-40nm) at constant edge length 100nm	117
<b>6.3</b>	Absorption efficiency of Al nanoprism for varying prism height (5-40nm) at constant edge length 150nm	119
<b>6.4</b>	Absorption efficiency of Al nanoprism for varying edge length (25-140nm) at constant prism height 15nm	120
<b>6.5</b>	Electric field intensity of Al nanoprism for varying prism height (5-100nm) at constant edge length 100nm	121

<b>6.6</b>	Electric field intensity of Al nanoprism for varying edge length (45-140nm) at constant prism height 15nm	122
------------	--	-----

## List of Tables

<b>Table Number</b>	<b>Description</b>	<b>Page Number</b>
1.1	Resonance conditions for different geometries	9
1.2	Values of different parameters for various metals	18
4.1	SPR peak position with extinction magnitude for Au, Ag and Al nano geometries embedded in perovskite medium	70

## **ABBREVIATIONS**

SPP	Surface Plasmon Polariton
SPPs	Surface Plasmon Polaritons
LSPR	Localized Surface Plasmon Resonance
MNP	Metal Nanoparticle
MNPs	Metal Nanoparticles
SP	Surface Plasmon
LSP	Localized Surface Plasmon
SPR	Surface Plasmon Resonance
DDA	Discrete Dipole Approximation
FDTD	Finite-Difference Time Domain
FEM	Finite Element Method
HNP	Hexagonal Nanoprism
Au	Gold
Ag	Silver
Al	Aluminium
Si	Silicon
SiO <sub>2</sub>	Silicon Dioxide
Au@SiO <sub>2</sub>	Core shell nanostructure made up of Au core and SiO <sub>2</sub> shell
CH <sub>3</sub> NH <sub>3</sub> PbI <sub>3</sub>	Methyl Ammonium Lead Iodide